Journal of Chromatography B 1060 (2017) 15–21

Contents lists available at ScienceDirect

Journal of Chromatography B

journal homepage: www.elsevier.com/locate/jchromb

Cross-platform metabolomics investigating the intracellular metabolic alterations of HaCaT cells exposed to phenanthrene

Guoting Jiang, Hongyan Kang, Yunqiu Yu*

School of Pharmacy, Fudan University, Shanghai, 201203, China

ARTICLE INFO

Keywords:
Metabolomics
Cross-platform
HaCaT cells
Phenanthrene

ABSTRACT

Phenanthrene (Phe) is one of the most abundant Polycyclic aromatic hydrocarbons (PAHs) contamination from various ambient sources, which has a tremendous impact on public health. However, our knowledge regarding its effects on skin remains limited. In this study, we investigated the metabolite profiling of the human keratinocytes HaCaT cells after Phe exposure to understand the toxic effects of Phe exposure on skin. To obtain a broad picture of metabolome with various hydrophilicity, a cross-platform approach with GC–MS and UHPLC–QTOF-MS has been employed. Data were analyzed by multivariate statistical analysis and samples were separated successfully using supervised PLS-DA models. It was shown that the impacts of Phe exposure on HaCaT cells were both dose-related and time-related. A total of 48 Phe-regulated metabolites were identified and among which 19 were confirmed by reference standards. By pathway analysis, amino acid metabolism, glutathione metabolism and glycerophospholipid metabolism were highlighted as the major metabolic pathways disturbed by Phe. Furthermore, it was found that the mechanisms included a reduced amino pool and a reduced antioxidant status. Overall, these results aid in improving understanding of the dermal toxicology related to Phe, and demonstrate this cross-platform approach is suitable for metabolomics researches on HaCaT cells.

1. Introduction

Environmental pollution has increasingly become the focus of attention. Polycyclic aromatic hydrocarbons (PAHs) are ubiquitous environmental pollutants that are mainly generated in incomplete combustion progress [1,2]. Phenanthrene (Phe) is one of the most abundant PAHs in the atmosphere [3], soil [4], aquatic environment [5], and even food [6]. Therefore, humans contact Phe in their daily life easily. Phe is also listed as one of the 16 priority PAHs by US Environmental Protection Agency. Numerous studies have unmasked the deleterious effects of Phe on internal organs [7–9], but our knowledge regarding its effects on skin remains limited. It was reported that the phototoxicity of Phe would increase γ-H2AX positive HaCaT cells [10]. And Phe exposure could influence the cytogenetic stability of dermal fibroblasts and increase the DNA damages [11]. However, there are rare literatures reported which focused on the metabolite profiling alterations of skin models exposed to Phe.

Metabolomics is a multidisciplinary science, which aims to measure downstream products present in biofluids, proposed in the late 1990s [12,13] and has been widely used in the research of diagnosing pathology and compound toxicity [14,15]. It's one of the "omics" technologies alongside genomics, transcriptomics and proteomics as an important platform for the research of global systems biology [16]. It was recently reported that environmental PAHs exposure causes oxidative stress-related effects in humans through a metabolomics research. However, there are other redox-active toxicants which may also contribute to the metabolic alterations [17]. Compared to animal models or human subjects, cell line applications offer advantages including easily controlled variables, lower cost, greater reproducibility, and easily interpreted results [18]. For this reason, the present study was designed to investigate metabolomics alterations in HaCaT cells, a widely applied *in vitro* skin keratinocytes paradigm owing to its highly preserved differentiation capacity [19], following Phe exposure using an untargeted metabolomics approach.

Mass spectrometry is a major analytical techniques used in metabolomics owing to its high sensitivity. Combination with a chromatographic separation reduces the complexity of the mass spectra and minimizes matrix effects due to metabolite separation in a time dimension [20,21]. GC–MS with electron ionization (EI) offers high sensitivity and reproducibility, and capability to identify unknowns with the established database. However, GC–MS is limited to the analysis of small volatile molecules and molecules that can be made volatile [22]. And the application of GC–MS alone would imply the inevitable loss of information of various ionic or nonvolatile metabolites.

* Corresponding author.
E-mail address: yqyu@shmu.edu.cn (Y. Yu).

http://dx.doi.org/10.1016/j.jchromb.2017.05.023
Received 28 January 2017; Received in revised form 24 April 2017; Accepted 22 May 2017
Available online 23 May 2017

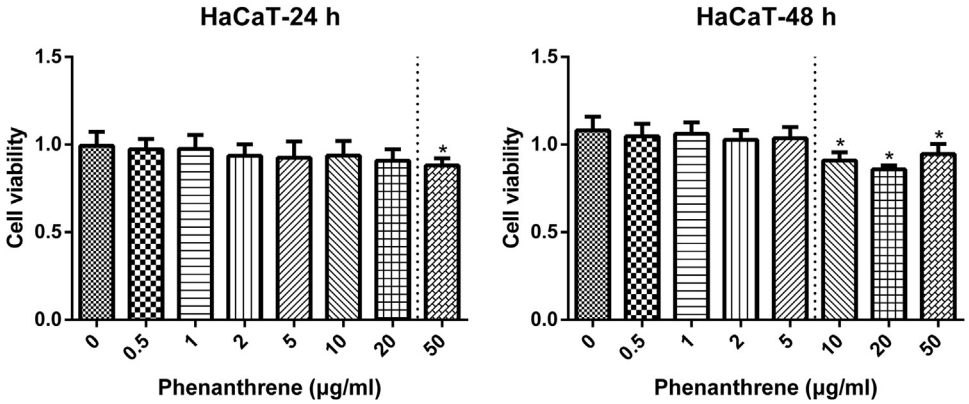

Fig. 1. Dose-response of HaCaT cells to Phe exposure in cell viability at 24 or 48 h. Cells were exposed to various concentrations of Phe (0–50 μg/mL) in DMEM and CCK-8 assay was used to analyze cell viability.

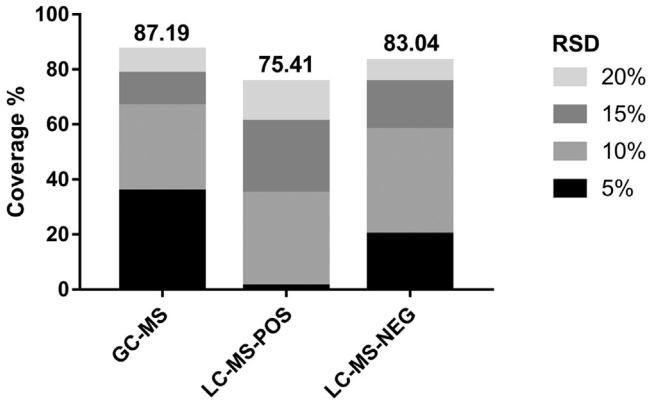

Fig. 2. Features coverage at different RSD level.

As a consequence, cross-platform approaches have been applied in metabolomics to increase the metabolome coverage [23,24]. UHPLC–QTOF-MS is an ideal complementary analytical technique to GC–MS and wildly used in metabolomics research. UHPLC method provides superior resolution and TOF detector affords high-resolution accurate mass (HRAM) data. In this study, cross-platform metabolomics with GC–MS and UHPLC–QTOF-MS was employed to research the dermal toxicology of Phe exposure on HaCaT cells for the first time. Cell metabolomics offered an overall picture of metabolome, while excluding the effects of unconcerned factors on the experimental results. The cross-platform strategy provided a higher metabolome coverage, which makes the global metabolite profiling more meaningful and reliable.

2. Materials and methods

2.1. Cell culture

HaCaT cells were purchased from American Type Culture Collection (ATCC) and cultivated in High Glucose DMEM medium (BasalMedia, China) supplemented with 10% Fetal bovine serum (FBS, Sigma-Aldrich, USA) and 1% penicillin-streptomycin solution (HyClone, USA), then incubated at 37 °C and 5% CO_2. Prior to the experiment, cells were seeded in 10 cm dishes at a density of 1×10^5 cells/mL.

2.2. Cell viability assay

To investigate the toxicity of Phe, cell viability was evaluated using

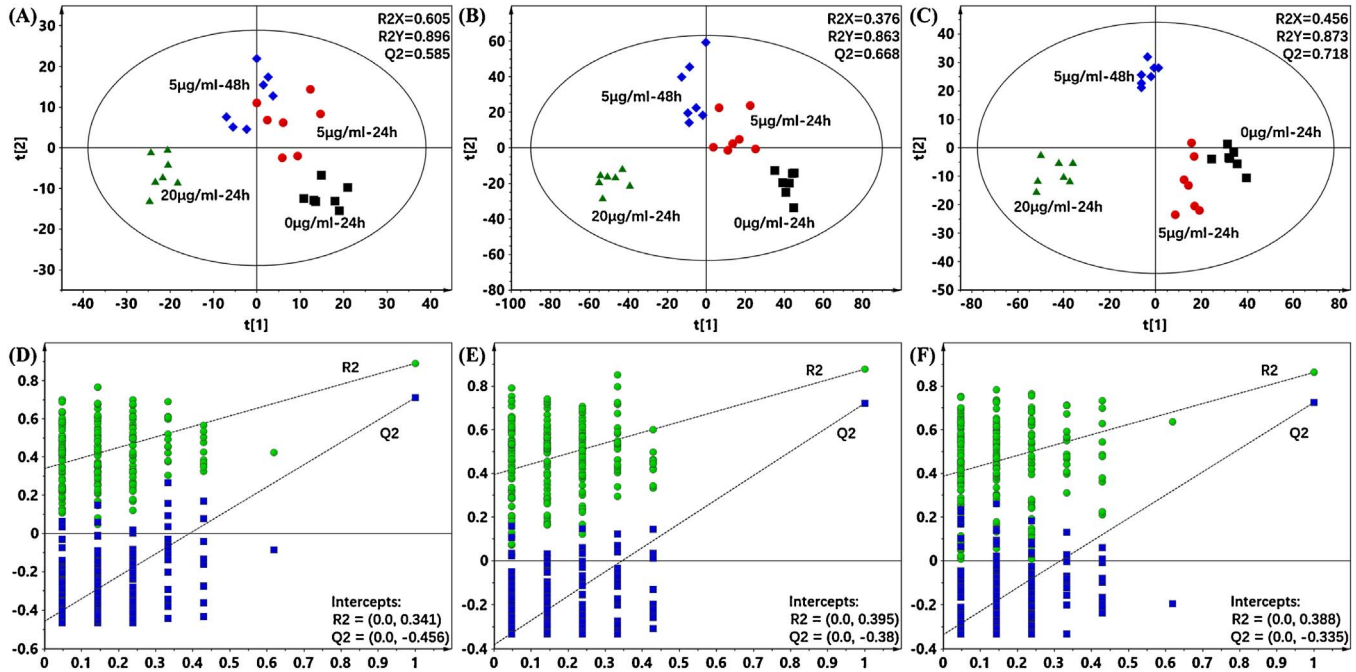

Fig. 3. PLS-DA scores plots for GC–MS (A), UHPLC-QTOF-POS (B), UHPLC-QTOF-NEG (C) data. The quality was validated by 200 permutation tests ((D) for GC–MS, (E) for UHPLC-QTOF-POS, (F) UHPLC-QTOF-NEG, respectively).

Table 1
Identification of differential metabolites by GC–MS.

HMDB ID	Metabolite	VIP	p value	Regulation
HMDB00191	L-Aspartic acid	1.23	7.49E − 08	down
HMDB00187	L-Serine*	1.16	2.37E − 12	down
HMDB00687	L-Leucine*	1.12	2.37E − 14	down
HMDB00172	L-Isoleucine*	1.12	1.30E − 14	down
HMDB01414	Putrescine	1.12	4.72E − 12	down
HMDB00161	L-Alanine*	1.14	3.51E − 13	down
HMDB00167	L-Threonine*	1.09	1.24E − 09	down
HMDB00883	L-Valine*	1.09	1.43E − 13	down
HMDB00158	L-Tyrosine*	1.08	5.70E − 11	down
HMDB00159	L-Phenylalanine*	1.10	9.99E − 13	down
HMDB00148	L-Glutamic acid*	1.29	1.43E − 08	down
HMDB00156	L-Malic acid*	1.07	1.95E − 08	down
HMDB00267	Pyroglutamic acid*	1.19	1.07E − 12	down
HMDB00094	Citric acid*	1.06	8.54E − 08	down
HMDB00162	L-Proline*	1.52	4.47E − 06	down
HMDB00123	Glycine*	1.02	2.24E − 07	down
HMDB01147	Aminomalonic acid	1.07	4.20E − 02	down
HMDB00190	L-Lactic acid*	1.16	8.39E − 04	up
HMDB00211	Myoinositol*	1.63	1.31E − 08	up
HMDB00224	*O*-Phosphoethanolamine*	1.32	2.53E − 12	up

*Identified by reference standard.

cell Counting Kit-8 (CCK-8, Dojindo Laboratories, Japan) according to the manufacturer's introductions. Briefly, HaCaT cells were seeded at a density of 1×10^4 per well (100 μL) in 96-well plates (Costar, USA). After 24-h incubation, the cells were treated with Phe (Aladdin Industrial Corporation, China) at various concentrations (0, 0.5, 1, 2, 5, 10, 20, 50 μg/mL) for 24 h and 48 h. Then, 10 μL of CCK8 was added to each well, and cells were incubated for 1 h at 37 °C. The absorbance was determined at 450 nm using Infinite 200 PRO microplate reader (Tecan Austria GmbH, Austria) and statistical analysis was performed using GraphPad Prism 7 (GraphPad Software, USA).

2.3. Phe exposure

Cells achieved 80% confluency after 48-h incubation in 10 cm dishes, and Phe was administered to final concentrations of 5, 20 μg/mL by adding 10 μL of solutions of 5, 20 mg/mL of Phe in DMSO (Sigma-Aldrich, USA) to 10 mL of medium. In addition to these 2 concentrations, a control group was used which involved the application of DMSO only at the same volume. Seven replicates were done for each exposure group and the control.

2.4. Cell quenching and metabolite extraction

After exposure, the medium was discarded and cells were washed with 10 mL room temperature phosphate buffer solution (PBS, BasalMedia, China), rather than ice cold PBS, in order to reduce temperature shock to the cells [25]. Then, the plates were quenched by directly adding ~15 mL of liquid nitrogen to the dish [26]. The plates were briefly stored on dry ice, transferred to a −80 °C freezer until extracted and assayed.

For extraction, 1.5 mL of ice-cold methanol containing 20 μg/mL tridecanoic acid (Sigma-Aldrich, USA) as internal standard was added to each plate and cells were detached from the surface with a disposable cell scraper (Crystalgen, China) and collected into a centrifuge tube for extraction. Cell lysates were then prepared with 10 min ultrasonication and 30 min incubation on ice. After centrifugation at 10,000*g* for 10 min, supernatant was divided into two portions, each 700 μL, and dried under the nitrogen stream at 40 °C.

2.5. Derivatization for GC–MS analysis

A two-stage chemical derivatization was performed on the dried extract. The dried samples were dissolved in 50 μL of pyridine (Sigma-Aldrich, USA) containing 15 mg/mL of methoxyamine hydrochloride (Sigma-Aldrich, USA), and were incubated at 40 °C for 2 h. After the oximation, samples were derivatized with 40 μL of MSTFA (*N*-Methyl-

Table 2
Identification of differential metabolites by UHPLC–QTOF-MS.

HMDB ID	Metabolite	Adduct	Measured MW (Da)	Theoretical MW (Da)	MW error (mDa)	VIP	p value	Regulation
HMDB07288	DG(18:3/20:5)	M+H	637.4811	637.482651	1.6	1.11	3.58E − 05	down
HMDB04078	Cinnavalininate	M+H	301.0465	301.045512	1.0	1.35	6.07E − 10	down
HMDB09147	PE(18:3/16:0)	M+H	698.5098	698.511916	2.1	1.12	7.65E − 04	down
HMDB08829	PE(14:0/18:2)	M+H	688.4886	688.491181	2.6	1.19	2.95E − 03	down
HMDB00318	3,4-Dihydroxyphenylglycol	M+H	171.0655	171.065185	0.3	1.51	5.70E − 10	down
HMDB00014	Deoxycytidine*	M+H	228.0974	228.097882	0.5	1.33	2.08E − 06	down
HMDB01191	dUTP	M+H	468.9800	468.980889	0.9	1.11	2.05E − 03	down
HMDB04224	N-(o)-Hydroxyarginine	M+H	191.1133	191.113866	0.6	1.11	4.06E − 03	down
HMDB01545	Pyridoxal	M+H	168.0663	168.065519	0.8	1.44	8.57E − 05	down
HMDB10408	LysoPC(18:1)	M+H	506.3624	506.360501	1.9	1.11	2.11E − 03	down
HMDB08836	PE(14:0/20:3)	M+H	714.5048	714.506831	2.0	1.20	4.88E − 02	down
HMDB12156	3-Isopropylmalate	M+H	177.0756	177.075749	0.1	1.26	1.06E − 02	down
HMDB56211	DG(18:1/0:0/18:4)	M+H	615.4971	615.498301	1.2	1.09	3.32E − 02	up
HMDB00905	2'-dAMP*	M+H	332.0768	332.075446	1.4	1.13	7.39E − 04	up
HMDB13410	PC(16:1/14:1)	M+H	688.5295	688.527566	2.0	1.14	4.82E − 02	up
HMDB60057	CE(15:0)	M+H	611.5760	611.576158	0.2	1.13	6.92E − 03	up
HMDB01066	S-Lactoylglutathione	M-H	378.0980	378.0977	0.4	1.21	2.16E − 13	down
HMDB09950	PIP(18:0/18:1)	M-H	943.5287	943.5318	3.1	1.16	9.30E − 05	down
HMDB01163	GDP-mannose	M-H	604.0695	604.0699	0.4	1.20	1.23E − 07	down
HMDB06779	Indole-5,6-quinone	M-H	146.0244	146.0248	0.4	1.27	2.91E − 08	down
HMDB11640	2',3'-Cyclic UMP	M-H	305.0169	305.0180	1.1	1.23	2.24E − 02	up
HMDB10383	LysoPC(16:1)	M-H	492.3074	492.3096	2.1	1.28	1.54E − 02	up
HMDB10380	LysoPC(14:1)	M-H	464.2778	464.2783	0.4	1.18	2.71E − 02	up
HMDB11472	LysoPE(0:0/15:0)	M-H	438.2621	438.2626	0.5	1.59	4.90E − 05	up
HMDB01278	Presqualene diphosphate	M-H	585.3095	585.3116	2.0	1.41	2.61E − 09	up
HMDB09939	PIP(16:1/16:1)	M-H	885.4555	885.4536	2.0	1.10	3.05E − 09	up
HMDB07867	PC(14:0/14:1)	M-H	674.4769	674.4766	0.3	1.07	7.86E − 08	up
HMDB29205	lysoPC(26:0)	M-H	634.4847	634.4817	3.0	1.14	4.07E − 11	up

*Identified by reference standard.

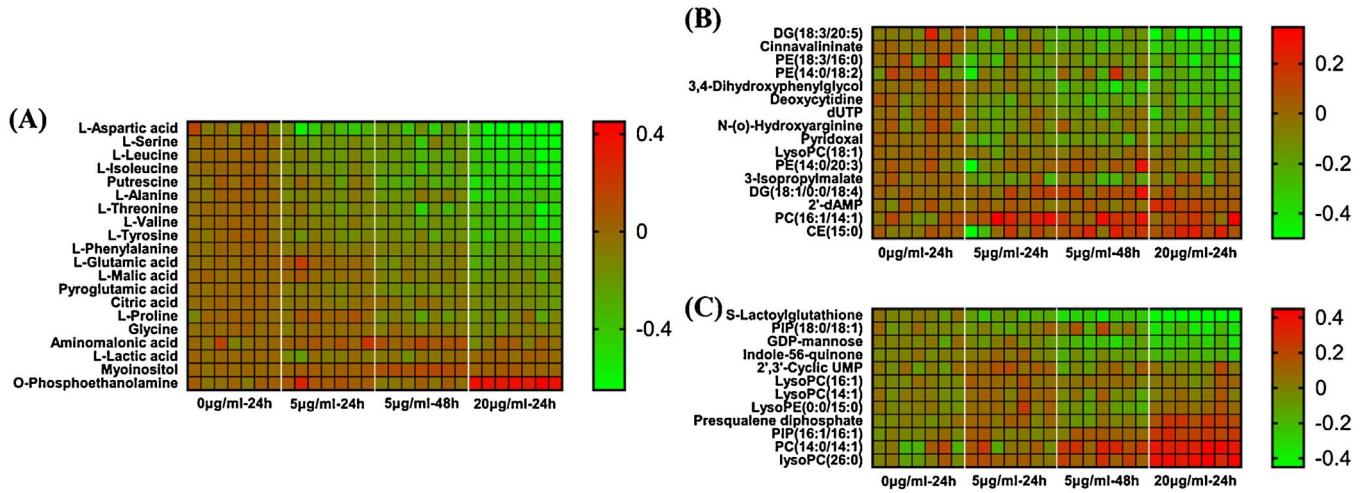

Fig. 4. Heat maps of identified metabolites analyzed using GC–MS (A), UHPLC-QTOF-POS (B) and UHPLC-QTOF-NEG (C). The ratio of metabolites in the exposure groups to average of those in controls samples were first calculated, and then the metabolic alterations were demonstrated as log10 (ratio).

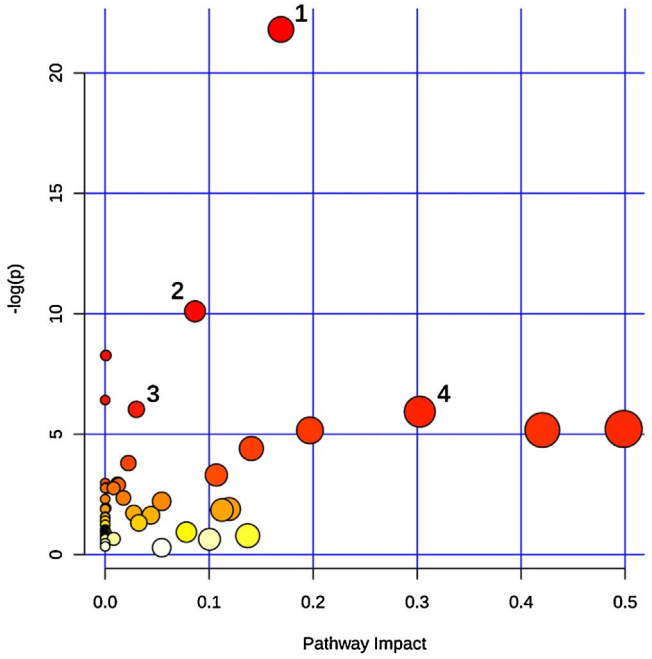

Fig. 5. Summary of metabolic pathways analyzed by MetaboAnalyst software. 1, Aminoacyl-tRNA biosynthesis; 2, Valine, leucine and isoleucine biosynthesis; 3, Glutathione metabolism; 4, Glycerophospholipid metabolism.

N-(trimethyl-silyl)trifluoroacetamide, ≥98.5%, Sigma-Aldrich, USA) under 40 °C for 1 h. After the silylation reaction, the solution was centrifuged at 10,000*g* for 10 min and the supernatant was analyzed using GC–MS.

2.6. GC–MS analysis

Derivatized samples were analyzed using the GC–MS system with a 7890 B gas chromatograph and 7693 autosampler coupled to a 5977A quadrupole mass analyzer (Agilent, USA) in full scan mode. Chromatographic separations were carried out on an HP-5 MS capillary column (30 m × 250 μm × 0.25 μm, Agilent, USA). Helium was used as a carrier gas at a flow rate of 1.2 mL/min and the inlet temperature was set at 300 °C. The inject volume and split ratio were set to 1 μL and 20:1. The temperature of the GC oven was set as follows: start at 70 °C, held for 3 min, then ramped at 5 °C/min up to 300 °C and held for 5 min. The temperatures of interface and ion source were set at 280 and 230 °C, respectively. Mass scanning in EI (electron impact) mode was carried out for the range of 33–600 *m/z* at a scan speed of 3125 u/s by MassHunter Acquisition Software (Agilent, USA) after 6.0 min of solvent delay. The detector voltage was set at 1.5 kV and the setting of EI ionization source was 70 eV. Samples of different groups were processed randomly.

2.7. UHPLC–QTOF-MS analysis

The dried samples were dissolved in 70 μL of methanol and centrifuged at 10,000*g* for 10 min. And the supernatant was analyzed with an UHPLC–QTOF-MS system. Chromatographic separation was performed on a 1260 Infinity UHPLC system (Agilent, USA) with an ACQUITY UPLC HSS T3 column (2.1 × 100 mm, 1.8 μm, Waters, USA). The inject volume was 5 μL and column temperature was 35 °C. For each sample, the run time was 27 min at a flow rate of 0.3 mL/min. The mobile phases were (A) H_2O with 0.1% formic acid and (B) acetonitrile with 0.1% formic acid. The programmed gradient was 0 min, 99% A; 1 min, 99% A; 5 min, 60% A; 8 min, 50% A; 10 min, 35% A; 16 min, 24% A; 20 min, 0% A; 25 min, 0% A; 27 min, 99% A with a 5 min post run.

The eluted metabolites were analyzed by a 6520 QTOF-MS (Agilent, USA) in electrospray ionization (ESI) positive and negative mode with a scan range of 50–1000 *m/z*. Capillary voltage was set at 3.5 kV and nebulizer pressure at 40 psi. Nitrogen was used as desolvation gas at a flow rate of 10 L/min at 350 °C. Data were collected in centroid mode. All samples were run in a random sequence.

2.8. Data processing

Raw data were transformed to mzData by MassHunter Qualitative Analysis B.06.00 (Agilent technologies, USA) and uploaded to XCMS online (https://xcmsonline.scripps.edu). Peak alignment, retention time correction and relative quantification of metabolite profiling were performed using this web-based software. And a two dimensional data table of ion peaks (retention time and *m/z*) and their intensities was generated [27]. Afterwards, "80 rule" [28] was employed for the peak filtering. Multivariate data analysis was performed using the program SIMCA 13 (Umetrics, Sweden). An unsupervised model, principal components analysis (PCA), was first performed to visualize the distribution of control and exposed groups, followed by supervised models including partial least squares-discriminant analysis (PLS-DA) to enhance separation and screen biomarkers. Furthermore, 200 times of permutation test cross validation was performed to ensure the suitability of the model.

The discriminating metabolites were selected according to the

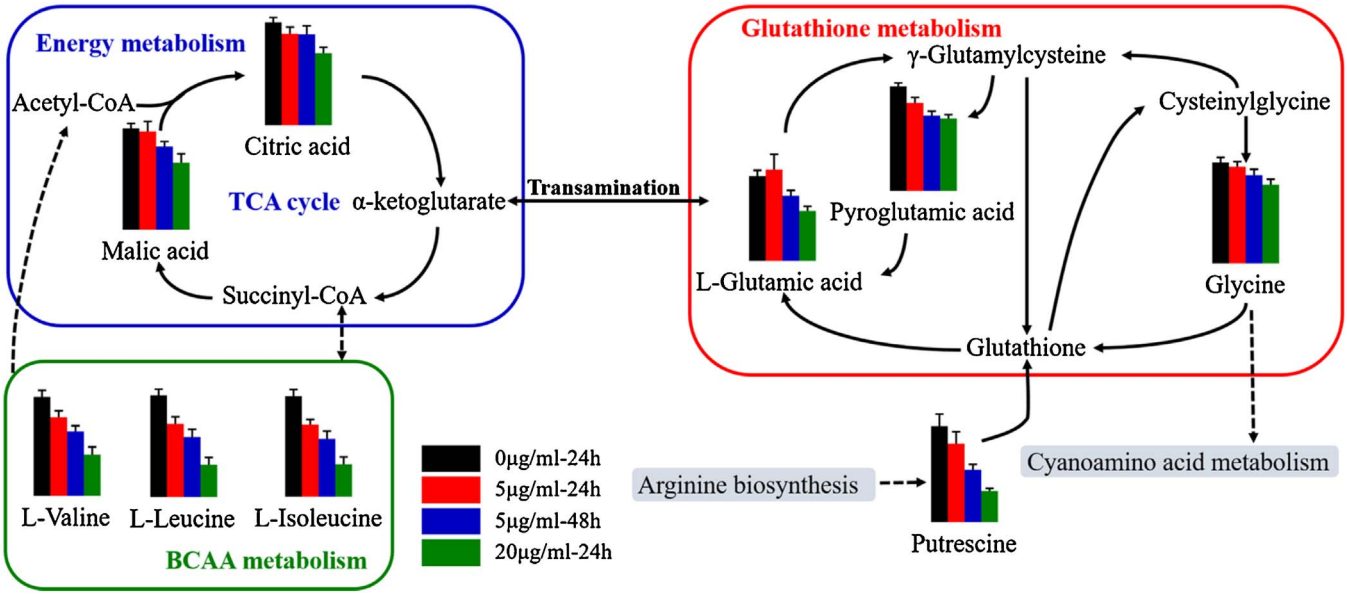

Fig. 6. Schematic representation of altered metabolic pathways. The column values in histograms were expressed as mean ± SD of their relative levels.

variable importance in projection (VIP) obtained from the PLS-DA model, which should be higher than 1. And one-way ANOVA with Duncan test was performed to determine whether levels of biomarker candidates identified using PLS-DA modeling were statistically significant between groups at the univariate analysis level. A p value ≤ 0.05 was considered statistically significant.

Next, the discriminating metabolites selected from GC–MS data were identified by combining NIST database and the Human Metabolome Database (HMDB, http://www.hmdb.ca) [29]. Metabolites identification of UHPLC–QTOF-MS was carried out by searching HMDB and METLIN (https://metlin.scripps.edu) based on the accurate mass number. Matches are approved at a mass error of less than 5 ppm. Furthermore, some metabolites were confirmed by comparing with reference standards. Heat map employing GraphPad was carried out to visualize the metabolic alterations of the discriminating metabolites. The identified marker metabolites were mapped through their respective metabolic pathways using MetaboAnalyst 3.0 (http://www.metaboanalyst.ca) [30].

3. Results

3.1. Effects of Phe on cell viability

To examine the cellular toxicity effect by Phe, CCK-8 assay was performed with serial concentrations of Phe, from 0.5 to 50 μg/mL, for 24 and 48 h. For the 24 h groups, 0.5–20 μg/mL did not affect the cell viability, while 50 μg/mL significantly reduced cell viability. In addition, for the 48 h groups, 10–50 μg/mL exposure had significant disturbances (Fig. 1). Therefore, cells were exposed to Phe at 5, 20 μg/mL for 24 h and 5 μg/mL for 48 h in this study, at non-cytotoxic doses.

3.2. Quality control

Quality control (QC) samples were prepared by mixing aliquots of each sample, and injected at an interval of 10 samples. After peak filtering and normalization, the RSD of peak intensity was calculated to represent the repeatability. A RSD of 20% could cover 87.19% features in GC–MS, 75.41% and 83.04% in UHPLC–QTOF-MS positive and negative mode (Fig. 2), respectively. Therefore, the results indicate that the present methods had good repeatability. In addition, the QC data clustered tightly together in the PCA scores plots (Fig. S1) indicating the acquired data are robust and worth further study.

3.3. Multivariate statistical analysis

PCA scores plots showed a tendency of separation of 4 groups in all three analytical methods (Fig. S2). All exposure groups were significantly distinguished on the first two component PLS-DA scores plots (Fig. 3A–C). In permutation test, models are considered valid for their ability to describe variation when the y intercept of R2 is < 0.3–0.4, and the predictive ability is considered valid when the y intercept of Q2 is < 0.05. [31] The parameters obtained from permutation test met the validation criteria (Fig. 3D–F), indicating that the PLS-DA models was not over-fitted and had reliable predictive ability.

3.4. Biomarker identification

Strict criteria were adopted in the screening: (1) VIP value > 1; (2) statistically significant (p value < 0.05) differences of metabolite contents (relative peak intensities) among the groups. After the screening and identification of candidates from the HMDB and METLIN databases, 20, 16 and 12 metabolites were annotated in the GC–MS, UHPLC–QTOF-MS positive and negative ion modes (Tables 1 and 2), respectively. Among these, 17 GC-metabolites and 2 LC-POS-metabolites were confirmed by the reference standards. As expected, most of GC-metabolites are amino acid while LC-metabolites are more lipophilic.

The overall metabolic alterations in different concentration Phe exposure and control group were visualized in the heat map. The heat map was plotted in a green-red color scale with red indicating an increase and green indicating a decrease of metabolite level. As shown in Fig. 4, the abundance of these metabolites presented a significant trend related to the exposure dose and time.

3.5. Metabolic pathway analysis

The HMDB IDs of differential metabolites were imported into the MetaboAnalyst 3.0. As a result, the web-based software generated 4 metabolic pathways with a FDR p value < 0.05, which were supposed to be significantly altered upon Phe exposure. These 4 pathways were characterized as (1) aminoacyl-tRNA biosynthesis, (2) valine, leucine and isoleucine biosynthesis, (3) glutathione metabolism, and (4) glycerophospholipid metabolism (Fig. 5). In brief, amino acid metabolism, glutathione metabolism and glycerophospholipid metabolism were the three major metabolic pathways disturbed by Phe in HaCaT cells.

4. Discussion

In this study, we investigated the influence of Phe exposure on the metabolite profiling of HaCat cells using GC–MS combined UHPLC–QTOF-MS analysis. The results showed that the metabolic alterations induced by Phe exposure were both dose-related and time-related. 48 Phe-regulated metabolites were identified and 19 were confirmed by reference standards. The amino acid pool was reduced after Phe exposure as shown in Table 1. The heat map showed the abundance of these metabolites presented a significant trend related to the exposure level. The perturbed metabolic pathways of HaCaT cells after Phe exposure were summarized in Fig. 6.

4.1. Effects on amino acid metabolism

As the result shown, the biosynthesis of branched chain amino acids (BCAA) were significantly influenced by Phe exposure. All three BCAA including valine, leucine and isoleucine were downregulated in response to Phe exposure. Consistent with our results, a decrease in valine was observed in an in vivo study of the alterations of mice plasma metabolites following PAHs exposure via PAHs-polluted water [32]. Previous studies demonstrated that BCAA could activate mammalian target of rapamycin (mTOR), which regulates protein synthesis and cell growth [33,34]. Combined with the result of cell viability assay, it could be concluded that Phe exposure could restrain the proliferation of HaCaT cells. Moreover, lower expression levels of metabolites in the TCA cycle, such as citric acid and L-malic acid, were consistent with a decreased availability of amino acids entering the cycle via transamination.

4.2. Effects on glutathione metabolism

The decrease of pyroglutamic acid, glycine, L-glutamic acid and putrescine indicated the disturbance of Phe exposure on glutathione metabolism. Pyroglutamic acid is a major intermediate metabolite in the γ-glutamyl cycle through which glutathione is synthesized and degraded [35,36], and it could be presumed that the biosynthesis of glutathione would also be reduced. In addition, it was reported that glutathione plays an important role in regulating redox states and scavenging reactive oxygen species (ROS) [37]. Therefore, a reduced antioxidant status was considered as part of biological effect of Phe exposure. Previous studies in vitro demonstrated that some toxicants, such as 2,3,7,8-tetrachlorodibenzo-*p*-dioxin (TCDD), airborne fine particulate matter (PM2.5), and Copper (Cu), downregulated glutamic acid [15,38,39]. Consistent with these reports, the cellular expression levels of glutamic acid after Phe treatment was significantly decreased. In addition, glutamic acid is a precursor of glutathione, α-ketoglutarate and ornithine [40] and it could thus be presumed that the biosynthesis of these compounds would also be reduced due to glutamic acid downregulation.

4.3. Effect on glycerophospholipid metabolism

Among these changed metabolites detected by UHPLC–QTOF-MS, amount of phosphatidylcholine (PC) and phosphatidylethanolamine (PE) were regulated after Phe exposure. Consistent with this result, the GC–MS result showed an increased in O-phosphoethanolamine, which is involved with glycerophospholipid metabolism. The combination of two analysis platforms had greatly increased the coverage of detected metabolites and validated the result of each other.

5. Conclusions

In this study, a cross-platform metabolomics approach was used to provide further insight into the metabolic response of HaCaT cells to Phe treatment. With the aid of multivariate analysis and metabolic pathway analysis, potential metabolite markers in the amino acid metabolism, glutathione metabolism, and glycerophospholipid metabolism were highlighted. The mechanisms included a reduced amino pool and a reduced antioxidant status. We believe that these results show how Phe affect our skin and more attention should be paid to our skin health as we exposed in a worse circumstance. Moreover, this cross-platform approach could obtain a broad picture of the hydrophilic and lipophilic metabolome in the study. And it's a useful tool for better understanding the metabolic changes in HaCaT cells during Phe exposure.

Acknowledgement

This study was funded by the 2015 Chinese Medical Association-Vichy research project (V2015110713).

Appendix A. Supplementary data

Supplementary data associated with this article can be found, in the online version, at http://dx.doi.org/10.1016/j.jchromb.2017.05.023.

References

[1] K. Ravindra, R. Sokhi, R. Vangrieken, Atmospheric polycyclic aromatic hydrocarbons: source attribution, emission factors and regulation, Atmos. Environ. 42 (2008) 2895–2921.
[2] E. Jang, M.S. Alam, R.M. Harrison, Source apportionment of polycyclic aromatic hydrocarbons in urban air using positive matrix factorization and spatial distribution analysis, Atmos. Environ. 79 (2013) 271–285.
[3] W.L. Ma, Y.F. Li, H. Qi, D.Z. Sun, L.Y. Liu, D.G. Wang, Seasonal variations of sources of polycyclic aromatic hydrocarbons (PAHs) to a northeastern urban city, China, Chemosphere 79 (2010) 441–447.
[4] B. Maliszewska-Kordybach, B. Smreczak, A. Klimkowicz-Pawlas, H. Terelak, Monitoring of the total content of polycyclic aromatic hydrocarbons (PAHs) in arable soils in Poland, Chemosphere 73 (2008) 1284–1291.
[5] W.J. Hong, H. Jia, Y.F. Li, Y. Sun, X. Liu, L. Wang, Polycyclic aromatic hydrocarbons (PAHs) and alkylated PAHs in the coastal seawater, surface sediment and oyster from Dalian, Northeast China, Ecotox. Environ. Safe. 128 (2016) 11–20.
[6] X. Duan, G. Shen, H. Yang, J. Tian, F. Wei, J. Gong, J.J. Zhang, Dietary intake polycyclic aromatic hydrocarbons (PAHs) and associated cancer risk in a cohort of Chinese urban adults: inter- and intra-individual variability, Chemosphere 144 (2016) 2469–2475.
[7] L. Huang, C. Wang, Y. Zhang, M. Wu, Z. Zuo, Phenanthrene causes ocular developmental toxicity in zebrafish embryos and the possible mechanisms involved, J. Hazard. Mater. 261 (2013) 172–180.
[8] S.K. Park, A.R. Ryu, M.Y. Lee, Protein expression profiling in the liver of rats exposed to phenanthrene, Mol. Cell. Toxicol. 9 (2013) 267–275.
[9] L. Huang, Z. Xi, C. Wang, Y. Zhang, Z. Yang, S. Zhang, Y. Chen, Z. Zuo, Phenanthrene exposure induces cardiac hypertrophy via reducing miR-133a expression by DNA methylation, Sci. Rep. 6 (2016) 20105.
[10] T. Toyooka, Y. Ibuki, New method for testing phototoxicity of polycyclic aromatic hydrocarbons, Environ. Sci. Technol. 40 (2006) 3603–3608.
[11] A. Mahvi, G. Mardani, P. Ghasemi-Dehkordi, J. Saffari-Chaleshtori, M. Hashemzadeh-Chaleshtori, M. Allahbakhshian-Farsani, N. Abdian, Effects of phenanthrene and pyrene on cytogenetic stability of human dermal fibroblasts using alkaline comet assay technique, Proc. Natl. Acad. Sci. India B: Biol. Sci. 85 (2015) 1055–1063.
[12] J.K. Nicholson, J.C. Lindon, E. Holmes, 'Metabonomics': understanding the metabolic responses of living systems to pathophysiological stimuli via multivariate statistical analysis of biological NMR spectroscopic data, Xenobiotica 29 (1999) 1181–1189.
[13] O. Fiehn, J. Kopka, P. Dormann, T. Altmann, R.N. Trethewey, L. Willmitzer, Metabolite profiling for plant functional genomics, Nat. Biotechnol. 18 (2000) 1157–1161.
[14] P. Dowling, M. Henry, P. Meleady, C. Clarke, K. Gately, K. O'Byrne, E. Connolly, V. Lynch, J. Ballot, G. Gullo, J. Crown, M. Moriarty, M. Clynes, Metabolomic and proteomic analysis of breast cancer patient samples suggests that glutamate and 12-HETE in combination with CA15-3 may be useful biomarkers reflecting tumour burden, Metabolomics 11 (2015) 620–635.
[15] Q. Huang, J. Zhang, L. Luo, X. Wang, X. Wang, A. Alamdar, S. Peng, L. Liu, M. Tian, H. Shen, Metabolomics reveals disturbed metabolic pathways in human lung epithelial cells exposed to airborne fine particulate matter, Toxicol. Res. 4 (2015) 939–947.
[16] S. Rochfort, Metabolomics reviewed: a new omics platform technology for systems biology and implications for natural products research, J. Nat. Prod. 68 (2005) 1813–1820.
[17] Z. Wang, Y. Zheng, B. Zhao, Y. Zhang, Z. Liu, J. Xu, Y. Chen, Z. Yang, F. Wang, H. Wang, J. He, R. Zhang, Z. Abliz, Human metabolic responses to chronic environmental polycyclic aromatic hydrocarbon exposure by a metabolomic

approach, J. Proteome Res. 14 (2015) 2583–2593.
[18] M. Cuperlovic-Culf, D.A. Barnett, A.S. Culf, I. Chute, Cell culture metabolomics: applications and future directions, Drug Discov. Today 15 (2010) 610–621.
[19] V.M. Schoop, N. Mirancea, N.E. Fusenig, Epidermal organization and differentiation of HaCaT keratinocytes in organotypic coculture with human dermal fibroblasts, J. Invest. Dermatol. 112 (1999) 343–353.
[20] K. Dettmer, P.A. Aronov, B.D. Hammock, Mass spectrometry-based metabolomics, Mass Spectrom. Rev. 26 (2007) 51–78.
[21] D.M. Drexler, M.D. Reily, P.A. Shipkova, Advances in mass spectrometry applied to pharmaceutical metabolomics, Anal. Bioanal. Chem. 399 (2011) 2645–2653.
[22] G.A. Theodoridis, H.G. Gika, E.J. Want, I.D. Wilson, Liquid chromatography–mass spectrometry based global metabolite profiling: a review, Anal. Chim. Acta 711 (2012) 7–16.
[23] S. Tufi, M.H. Lamoree, J. De Boer, P.E. Leonards, Cross-platform metabolic profiling: application to the aquatic model organism Lymnaea stagnalis, Anal. Bioanal. Chem. 407 (2015) 1901–1912.
[24] E.J. Gu, D.W. Kim, G.J. Jang, S.H. Song, J.I. Lee, S.B. Lee, B.M. Kim, Y. Cho, H.J. Lee, H.J. Kim, Mass-based metabolomic analysis of soybean sprouts during germination, Food Chem. 217 (2017) 311–319.
[25] K.A. Hollywood, C.L. Winder, W.B. Dunn, Y. Xu, D. Broadhurst, C.E. Griffiths, R. Goodacre, Exploring the mode of action of dithranol therapy for psoriasis: a metabolomic analysis using HaCaT cells, Mol. Biosyst. 11 (2015) 2198–2209.
[26] M.A. Lorenz, C.F. Burant, R.T. Kennedy, Reducing time and increasing sensitivity in sample preparation for adherent mammalian cell metabolomics, Anal. Chem. 83 (2011) 3406–3414.
[27] R. Tautenhahn, G.J. Patti, D. Rinehart, G. Siuzdak, XCMS Online: a web-based platform to process untargeted metabolomic data, Anal. Chem. 84 (2012) 5035–5039.
[28] S. Bijlsma, I. Bobeldijk, E.R. Verheij, R. Ramaker, S. Kochhar, I.A. Macdonald, B. van Ommen, A.K., Smilde, Large-scale human metabolomics studies: a strategy for data (pre-) processing and validation, Anal. Chem. 78 (2006) 567–574.
[29] D.S. Wishart, T. Jewison, A.C. Guo, M. Wilson, C. Knox, Y. Liu, Y. Djoumbou, R. Mandal, F. Aziat, E. Dong, S. Bouatra, I. Sinelnikov, D. Arndt, J. Xia, P. Liu, F. Yallou, T. Bjorndahl, R. Perez-Pineiro, R. Eisner, F. Allen, V. Neveu, R. Greiner, A. Scalbert, HMDB 3.0—the human metabolome database in 2013, Nucleic Acids Res. 41 (2013) D801–D807.
[30] J. Xia, I.V. Sinelnikov, B. Han, D.S. Wishart, Metabo analyst 3.0—making metabolomics more meaningful, Nucleic Acids Res. 43 (2015) W251–W257.
[31] U. Paolucci, K.E. Vigneau-Callahan, H. Shi, W.R. Matson, B.S. Kristal, Development of biomarkers based on diet-dependent metabolic serotypes: characteristics of component-based models of metabolic serotypes, OMICS 8 (2004) 221–238.
[32] Y. Zhang, B. Wu, X. Zhang, A. Li, S. Cheng, Metabolic profiles in serum of mouse after chronic exposure to drinking water, Hum. Exp. Toxicol. 30 (2011) 1088–1095.
[33] D.D. Sarbassov, S.M. Ali, D.M. Sabatini, Growing roles for the mTOR pathway, Curr. Opin. Cell Biol. 17 (2005) 596–603.
[34] C. Fumarola, S. La Monica, G.G. Guidotti, Amino acid signaling through the mammalian target of rapamycin (mTOR) pathway: role of glutamine and of cell shrinkage, J. Cell. Physiol. 204 (2005) 155–165.
[35] C.D. Pederzolli, A.M. Sgaravatti, C.A. Braum, C.C. Prestes, G.K. Zorzi, M.B. Sgarbi, A.T. Wyse, C.M. Wannmacher, M. Wajner, C.S. Dutra-Filho, 5-Oxoproline reduces non-enzymatic antioxidant defenses in vitro in rat brain, Metab. Brain Dis. 22 (2007) 51–65.
[36] A. Kumar, A.K. Bachhawat, Pyroglutamic acid: throwing light on a lightly studied metabolite, Curr. Sci. 102 (2012) 288–297.
[37] R. Masella, R. Di Benedetto, R. Vari, C. Filesi, C. Giovannini, Novel mechanisms of natural antioxidant compounds in biological systems: involvement of glutathione and glutathione-related enzymes, J. Nutr. Biochem. 16 (2005) 577–586.
[38] A. Ruiz-Aracama, A. Peijnenburg, J. Kleinjans, D. Jennen, J. van Delft, C. Hellfrisch, A. Lommen, An untargeted multi-technique metabolomics approach to studying intracellular metabolites of HepG2 cells exposed to 2,3,7,8-tetrachlorodibenzo-p-dioxin, BMC Genom. 12 (2011) 251.
[39] Y. Xiao, Q. Zhai, G. Wang, X. Liu, J. Zhao, F. Tian, H. Zhang, W. Chen, Metabolomics analysis reveals heavy metal copper-induced cytotoxicity in HT-29 human colon cancer cells, RSC Adv. 6 (2016) 78445–78456.
[40] H. Tapiero, G. Mathe, P. Couvreur, K.D. Tew, Dossier Free amino acids in human health and pathologies—II. Glutamine and glutamate, Biomed. Pharmacother. 56 (2002) 446–457.